Dissipation in Turbulent Plasma due to Reconnection in Thin Current Sheets

David Sundkvist,[1,*] Alessandro Retinò,[2] Andris Vaivads,[2] and Stuart D. Bale[1]
[1]*Space Sciences Laboratory, University of California, Berkeley, California, USA*
[2]*Swedish Institute of Space Physics, Uppsala, Sweden*
(Received 28 November 2006; published 13 July 2007)

We present *in situ* measurements in a space plasma showing that thin current sheets the size of an ion inertial length exist and are abundant in strong and intermittent plasma turbulence. Many of these current sheets exhibit the microphysical signatures of reconnection. The spatial scale where intermittency occurs corresponds to the observed structures. The reconnecting current sheets represent a type of dissipation mechanism, with observed dissipation rates comparable to or even dominating over collisionless damping rates of waves at ion inertial length scales (× 100), and can have far reaching implications for small-scale dissipation in all turbulent plasmas.

DOI: 10.1103/PhysRevLett.99.025004 PACS numbers: 52.35.Ra, 52.35.Vd, 52.72.+v

Turbulence is an inherently nonlinear phenomena of fluids and plasmas involving fluctuations over a wide range of scales. A well-known feature of turbulence for intermediate or high Reynolds numbers is the occurrence of spatial nonuniformity (intermittency) at certain scales. The intermittency is ascribed to the presence of coherent structures such as magnetic islands, localized magnetic flux tubes, vortex structures, etc. [1–3]. In an environment with strong intermittent magnetic turbulence thin current sheets develop spontaneously at the border between interacting magnetic flux tubes as observed in numerical simulations and noted in theory [4–8]. Thin current sheets have been widely observed in magnetospheric and laboratory plasmas and are associated with the process of magnetic reconnection [9–13]. Reconnection is a dissipative process which converts magnetic energy to kinetic and thermal particle energies. In this Letter we use space plasma as a turbulence laboratory and present evidence that coherent dissipation by reconnection in thin current sheets can be comparable to or dominating over traditional dissipation from collisionless Landau and cyclotron damping.

We analyze the strongly turbulent solar wind downstream of Earth's bow shock, the so-called magnetosheath, for the presence of intermittency together with thin current sheets showing the microphysical signature of reconnection. The plasma in this region is comprised of magnetic structures convected Earthward with the shocked solar wind, together with Alfvén/ion cyclotron waves [14–16]. We have analyzed Cluster spacecraft data [17] from the terrestrial magnetosheath on the 27 March 2002 from 09:30 UT to 11:45 UT. Spacecraft data were sampled in a burst mode with higher sampling rates, allowing us to reveal the details of the microphysics down to the ion inertial scale and smaller. We have used data from the EFW (electric field), FGM (magnetic field), and CIS (ions) experiments [17]. At 09:35 UT the spacecraft crossed the bow shock and entered the magnetosheath, see Fig. 1. The angle between the shock normal and the interplanetary magnetic field (IMF) obtained from the ACE spacecraft situated in the solar wind was ∼20°, and thus classifies this as quasiparallel bowshock conditions. From 09:35 to 11:00 the spacecraft stayed in the downstream quasiparallel region. At 11:00 the IMF changed significantly and transformed the conditions to a quasiperpendicular type. This temporal rather than spatial transition

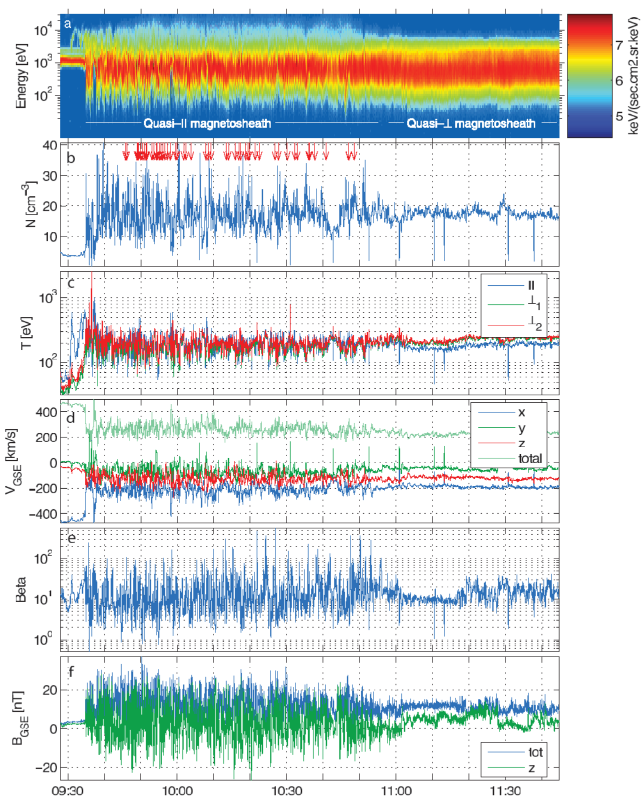

FIG. 1 (color). Overview of plasma parameters in the magnetosheath as observed by Cluster spacecraft 1 (C1). (a) Ion spectrogram, (b) density, (c) ion temperature, (d) ion velocity, (e) plasma beta, (f) magnetic field. The occurrence of thin current sheets for shear angle >120 degrees is shown with arrows in panel (b). See also Table I.

is clearly visible in Figs. 1(b), 1(d), and 1(f), showing a significant drop in fluctuation amplitude for the density, velocity, and magnetic fields, respectively. The plasma beta (β—ratio of plasma to magnetic pressure) is high on average in the downstream region [$\beta_p \approx 10$, Fig. 1(e)] because of the heating and compression of the plasma at the shock and the low average ambient magnetic field, but can locally be lower. The large amplitude magnetic field fluctuations $|\delta \mathbf{B}| \sim |\mathbf{B}|$, Fig. 1(f), are already in a strongly nonlinear stage, which make it difficult to classify them in terms of usual wave modes which are developed for small amplitude perturbations.

We performed a statistical search for thin current sheets in this strong turbulence. An event was classified as a current sheet if the magnetic shear angle between at least two spacecraft was large enough (we changed the minimum shear angle in intervals from 30 to 150 degrees), while at the same time the magnetic field was larger than 5 nT for at least one spacecraft. Since the spacecraft separation was less than $200\ \text{km} \sim 4\lambda_i$, where $\lambda_i \sim 50$ km is the average ion inertial length in the magnetosheath, we found current sheets with a typical thickness of a few λ_i. The number of thin current sheets found is displayed in Table I. The 55 current sheets with shear angle >120 degrees have been examined in more detail, and their location in the magnetosheath is indicated with red arrows in Fig. 1(b). More than half of these current sheets show the signs of reconnection at the time of crossing (nonzero magnetic field normal component and quadrupolar out-of-plane component, see Fig. 2 for definitions). An important result of the search is that thin current sheets are only found in the time interval corresponding to the region downstream of the quasiparallel shock. This is true regardless of shear angle. This might be because the turbulence is stronger and more developed downstream of the quasiparallel than the quasiperpendicular shock. We note that high-energy ions with energies above 20 keV are observed, Fig. 1(a), only in intervals where thin current sheets exist, Fig. 1(b). See the discussion below relating this to reconnection. A large fraction of the analyzed current sheets had a velocity (obtained from four-spacecraft timing) in the direction of but smaller than the magnetosheath flow speed $v_{\mathrm{cs}} \approx 150$–$200\ \text{km/s} < v_{\mathrm{MS}} \approx 250\ \text{km/s}$, indicating that the structures are propagating upstream in the plasma frame, reminiscent of short large-amplitude magnetic structures (SLAMS).

TABLE I. The number of thin current sheets found in the magnetosheath on 2002-03-27 as a function of magnetic shear angle.

Shear angle	Number of current sheets
>30	293[a]
>60	159[a]
>90	95[a]
>120	55
>150	30

[a]Calculated from an automatic analysis.

A subset of the measured parameters of one of the analyzed current sheets is shown in Fig. 2. The detailed analysis of the microphysics of the current sheet showing that it has the signatures of reconnection is discussed in [18]. Figure 2(a) shows a 10 s interval of the magnetic field together with the density fluctuations. The yellow patch shows the location of the analyzed current sheet analyzed in Figs. 2(b) and 2(c).

The labels L, M, and N in Fig. 2 refer to the maximum, intermediate, and minimum directions, respectively, obtained from a minimum variance analysis of the current sheet. Figure 2(b) shows the reconnecting component, the out-of-plane component, and the normal component of the magnetic field. These signatures are consistent with the spacecraft crossing the ion diffusion region during reconnection [18]. The $\mathbf{j} \cdot \mathbf{E} > 0$ in Fig. 2(c) is positive, meaning conversion of magnetic energy to thermal and kinetic particle energy, consistent with ongoing reconnection.

We now discuss the properties of the turbulent environment where these current sheets are formed. Figure 3 shows the power spectral density of the turbulent magnetic and electric field fluctuations, respectively. We used a 6 min. period centered at the location of the current sheet in Fig. 2. The electric field shown is the GSE_y component of the plasma rest frame electric field $\mathbf{E}'$, calculated using $\mathbf{E}' = \mathbf{E} - \mathbf{v}\mathbf{x}\mathbf{B}$, where $\mathbf{v}$ is the plasma bulk velocity and $\mathbf{E}$ the electric field as measured in the spacecraft frame. The E'_y/B_z ratio is close to the Alfvén speed $v_A \sim 87$ km/s in the low frequency limit, indicating that these fluctuations are Alfvénic or magnetosonic. As indicated in the figure, several characteristic ranges in frequency can be seen. For the magnetic field fluctuations we find the scaling $f^{-1.7}$ for $f \in [0.07, 0.3]$ Hz in what could be called the inertial range, and $f^{-3.1}$ for $f \in [0.7, 10]$ Hz, the MHD scale dispersion or dissipation range. The slope -1.7 is close

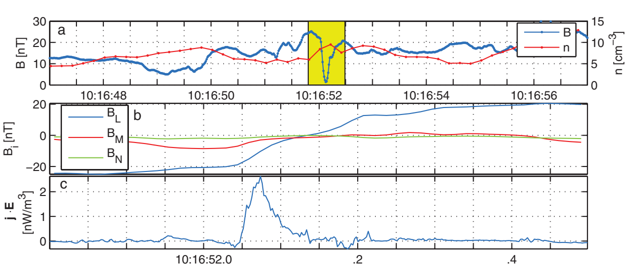

FIG. 2 (color). Microphysics of a thin current sheet in the magnetosheath observed by C4. The LMN-coordinate system is defined in the text. (a) Magnetic field and density fluctuations. The yellow patch is shown in detail in panels the panels below. (b) Reconnecting component of magnetic field (B_L), out-of-plane component (B_M), normal component (B_N). (c) Dissipated power per unit volume.

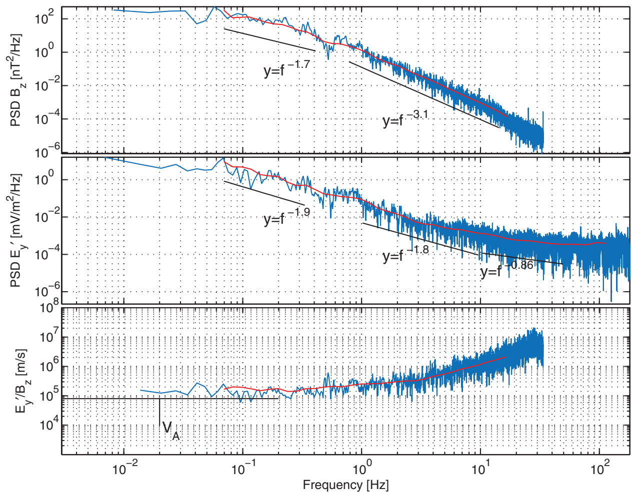

FIG. 3 (color). Power spectral density of the magnetic (top) and electric field (middle) from C3. The blue lines are calculated with a fast Fourier transform, while the red lines are obtained using a wavelet transform. The E_y'/B_z ratio in the plasma frame (bottom) is close to the Alfvén speed $v_A \sim 87$ km/s in the low frequency limit (black line). The slopes were calculated from a least squares fit to the spectrum (wavelet) for the respective frequency ranges and have been vertically shifted for clarity.

to the Kolmogorov value of $-5/3$. A recent Letter [19] reported a slightly different slope for the power law spectrum in another part of the magnetosheath, closer to the magnetopause. The electric field gets enhanced at smaller scales, similar to previous observations in the solar wind [20].

To check for the deviation from scale invariance (intermittency), a sign of presence of coherent structures, the probability distribution functions (PDFs) of the structure functions $S_p(\tau) = \langle |y(t+\tau) - y(t)|^p \rangle$ of magnetic field fluctuations were calculated. In Fig. 4(a) the PDFs of $y = B_z$ (often the reconnecting component) for $p = 1$ are shown for different time lags τ, corresponding to different spatial scales according to Taylor's hypothesis, i.e., assuming that the turbulence is frozen in the measured wave field and convected past the spacecraft. This is validated by noting that the sweeping speed $v_{\mathrm{MS}} \approx 250$ km/s is much greater than the dynamical speed $v_A \approx 87$ km/s. The PDFs are rescaled to unit standard deviation and zero mean. The black line in the figure is the theoretical result for a random Gaussian process. We note that deviation from a statistically independent process begins at scales slightly larger than the ion Larmor scale ($1s \sim 1\rho_i$) and continues through the ion inertial scale ($\lambda_i \sim 0.3\rho_i$). To quantify how the distribution of fluctuation amplitudes deviates from a Gaussian, we calculated the kurtosis as a continuous function of τ, shown in Fig. 4(b). For a Gaussian process the kurtosis, $K = \langle (y - \langle y \rangle)^4 \rangle / \langle (y - \langle y \rangle)^2 \rangle^2 - 3$, should be equal to zero. The intermittency starts at $\tau \sim 10$ s, corresponding approximately to $10\rho_i$, and the kurtosis increases before it flattens out at $\tau = 0.01$ s. While this behavior is general, the value of K for $\tau < 0.01$ s depends on the time interval chosen for the analysis. Intermittency has previously been reported both upstream and downstream of the bowshock [16], and more recently in the foreshock region [21].

To further quantify this intermittent behavior of the plasma with an independent check, the dimensionless structure functions $A_p(\tau) = S_p(\tau)/S_2(\tau)^{p/2}$ were calculated, with the result (normalized to a Gaussian) displayed in Fig. 4(c). The dimensionless structure functions should not depend on τ for a Gaussian process (e.g. [16]). From the figure it is seen that $A_p(\tau) \sim 1$ for $\tau > 10$ s, in agreement with the kurtosis, Fig. 4(b). From these two tests we draw the conclusion that intermittency at scales of a few ion Larmor radii and smaller is present in the plasma. These length scales correspond to the vicinity of the dispersion or dissipation range for the low frequency turbulence.

Since the observed $\mathbf{j} \cdot \mathbf{E} > 0$, Fig. 2(c), energy is transferred from stored magnetic energy to thermal and kinetic particle energies when the current sheets reconnect. There are basically three ways the energy can be converted: (1) local heating of the plasma. This is observed in the current sheets [18]. (2) High-energy tails of the distribution functions. We observe a clear correspondence between the presence of thin current sheets and high-energy ions, Fig. 1(a) and 1(b). Proton acceleration has been studied in reconnecting current sheets [22], also with effects from MHD turbulence [23], conditions similar to what is reported here. Fermi acceleration at the quasiparallel bow

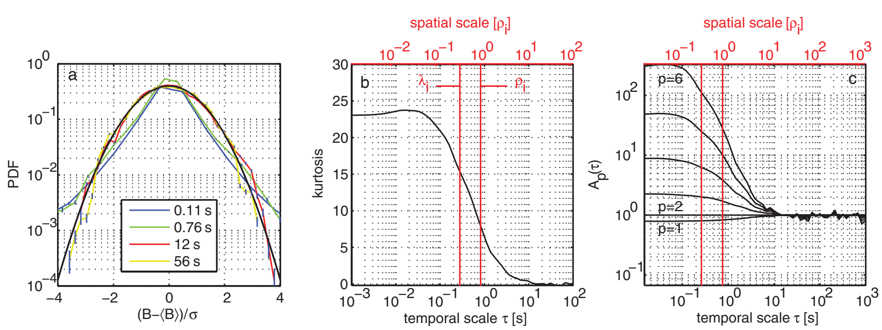

FIG. 4 (color). Analysis of the intermittent behavior of the strong turbulence, using magnetic field data from C4. (a) Probability distribution functions for B_z at indicated time lags τ. (b) Kurtosis as a function of the time lag τ. (c) Dimensionless structure functions $A_p(\tau)$ normalized to a Gaussian. The spatial scale is calculated from $v_{\mathrm{MS}} \cdot \tau$ (Taylor's hypothesis is assumed valid).

shock [24] is another possible cause for the high-energy ions, although we do not observe them at the immediate shock. Fermi acceleration through magnetic mirroring between the current sheets is another possible mechanism. (3) Kinetic energy in the form of reconnection jets. The jets cannot be resolved with the time resolution of the present instrumentation and will not be discussed further. In the strong turbulence in the magnetosheath, all these mechanisms lead to a general dissipation of magnetic energy localized to spatial scales comparable to the thickness of the current sheets around one ion inertial length. Previous studies in the solar wind [25,26] show that the onset of the dissipation range most likely occurs at the ion inertial length and suggests that reconnection in thin current sheets can provide an efficient channel for dissipation. The abundance of reconnecting thin current sheets reported here supports this picture. The demonstrated association of current sheets with intermittency and larger scale structures leads us to denote this as a coherent dissipation mechanism, representing *nonlocal* (in wave-number space) interactions of different scales. This is in contrast to classical dissipation scenarios manifested by, e.g., Landau or cyclotron damping.

We now estimate the relative importance of coherent dissipation to wave damping. The global coherent dissipation rate through reconnection $\langle w \rangle_{\mathrm{coh}}$ is dependent on the density of current sheets. For simplicity we assume steady state reconnection with all measured $\mathbf{j} \cdot \mathbf{E}$ dissipated. We then get the effective dissipation rate $\langle w \rangle_{\mathrm{coh}} \sim (V_{\mathrm{diss}}/V_{\mathrm{tot}}) \langle \mathbf{j} \cdot \mathbf{E} \rangle \sim (N\lambda_i/L) \langle \mathbf{j} \cdot \mathbf{E} \rangle \sim 10^{-12}\ \mathrm{W/m^3}$, where we have used a unit area with normal parallel to the flow, $N \approx 30$ is the number of reconnecting current sheets with shear $>120°$ from Table I, and $L = (250\ \mathrm{km/s})5400$ s, the flow velocity times the duration of observation of the current sheets from Fig. 1. The damping rate of fluctuations is $\langle w \rangle_{\mathrm{waves}} = \langle \partial_t (u_B + u_E) \rangle \sim 2 \langle \partial_t u_B \rangle = 4\gamma (\delta B)^2/(2\mu_0) \sim 10^{-14}\ \mathrm{W/m^3}$ with fluctuation energy from Fig. 3 and an average $\gamma/\Omega_{\mathrm{cp}} = -1$ for magnetosonic and Alfvén waves at wavelengths λ_i. We thus estimate $\langle w \rangle_{\mathrm{coh}} / \langle w \rangle_{\mathrm{waves}} \sim 10^2$ at scales λ_i. We conclude that dissipation in reconnecting current sheets can be a competing, or as here even dominating, source of energy dissipation in turbulent plasmas at ion inertial length scales. Waves, on the other hand, can be damped over larger intervals in wave-number space.

We thank S. C. Buchert and the FGM team for the magnetic field data and H. Nilsson and the CIS team for the particle data. We thank F. Mozer for help with calibrating the EFW data, the ACE/MAG team for use of IMF data, and the referees for useful suggestions. The research of D. S. was supported by NASA Grant No. NNG05GL27G. The research of A. R. was supported by the Swedish National Space Board. The research of A. V. is supported by the Swedish Research Council.

*sundkvist@ssl.berkeley.edu

[1] U. Frisch, *Turbulence: The Legacy of A. N. Kolmogorov* (Cambridge University Press, Cambridge, England, 1995).
[2] Y. Zhou, W. H. Matthaeus, and P. Dmitruk, Rev. Mod. Phys. **76**, 1015 (2004).
[3] D. Biskamp, *Magnetohydrodynamic Turbulence* (Cambridge University Press, Cambridge, England, 2003).
[4] W. H. Matthaeus and D. Montgomery, Annals New York Acad. Sci. **357**, 203 (1980).
[5] W. H. Matthaeus and D. Montgomery, J. Plasma Phys. **25**, 11 (1981).
[6] W. H. Matthaeus and S. L. Lamkin, Phys. Fluids **29**, 2513 (1986).
[7] V. Carbone, P. Veltri, and A. Mangeney, Phys. Fluids **2**, 1487 (1990).
[8] D. Tetreault, J. Geophys. Res. **97**, 8541 (1992).
[9] B. U. Ö. Sonnerup, *Magnetic Field Reconnection*, Solar System Plasma Physics Vol. 3 (North-Holland, Amsterdam, 1979).
[10] E. Priest and T. Forbes, *Magnetic Reconnection* (Cambridge University Press, Cambridge, England, 2000).
[11] F. S. Mozer, S. D. Bale, and T. D. Phan, Phys. Rev. Lett. **89**, 015002 (2002).
[12] A. Vaivads, Y. Khotyaintsev, M. André, A. Retinò, S. C. Buchert, B. N. Rogers, P. Décréau, G. Paschmann, and T. D. Phan, Phys. Rev. Lett. **93**, 105001 (2004).
[13] M. Øieroset, T. D. Phan, M. Fujimoto, R. P. Lin, and R. P. Lepping, Nature (London) **412**, 414 (2001).
[14] S. J. Schwartz, D. Burgess, and J. J. Moses, Ann. Geophys. **14**, 1134 (1996).
[15] D. Burgess, E. A. Lucek, M. Scholer, S. D. Bale, M. A. Balikhin, A. Balogh, T. S. Horbury, V. V. Krasnoselskikh, H. Kucharek, and B. Lembège *et al.*, Space Sci. Rev. **118**, 205 (2005).
[16] T. Dudok de Wit and V. V. Krasnosel'skikh, Nonlin. Proc. Geophys. **3**, 262 (1996).
[17] C. P. Escoubet, R. Schmidt, and M. L. Goldstein, Space Sci. Rev. **79**, 11 (1997).
[18] A. Retinò, D. Sundkvist, A. Vaivads, F. Mozer, M. André, and C. J. Owen, Nature Phys. **3**, 236 (2007).
[19] F. Sahraoui, G. Belmont, L. Rezeau, N. Cornilleau-Wehrlin, J. L. Pinçon, and A. Balogh, Phys. Rev. Lett. **96**, 075002 (2006).
[20] S. D. Bale, P. J. Kellogg, F. S. Mozer, T. S. Horbury, and H. Rème, Phys. Rev. Lett. **94**, 215002 (2005).
[21] Y. Narita, K.-H. Glassmeier, and R. A. Treumann, Phys. Rev. Lett. **97**, 191101 (2006).
[22] J. Heerikhuisen, Y. E. Litvinenko, and I. J. D. Craig, Astrophys. J. **566**, 512 (2002).
[23] P. Dmitruk, W. H. Matthaeus, and N. Seenu, Astrophys. J. **617**, 667 (2004).
[24] M. A. Lee, J. Geophys. Res. **87**, 5063 (1982).
[25] R. J. Leamon, C. W. Smith, N. F. Ness, W. H. Matthaeus, and H. K. Wong, J. Geophys. Res. **103**, 4775 (1998).
[26] R. J. Leamon, W. H. Matthaeus, C. W. Smith, G. P. Zank, D. J. Mullan, and S. Oughton, Astrophys. J. **537**, 1054 (2000).